Medicine®

OBSERVATIONAL STUDY

OPEN

Using Flat-Panel Perfusion Imaging to Measure Cerebral Hemodynamics

A Pilot Feasibility Study in Patients With Carotid Stenosis

Chung-Jung Lin, MD, Wan-Yuo Guo, MD, PhD, Feng-Chi Chang, MD, Sheng-Che Hung, MD, Ko-Kung Chen, PhD, Deuerling-Zheng Yu, PhD, Chun-Hsien Frank Wu, PhD, and Jy-Kang Adrian Liou, MSc

Abstract: Flat-detector CT perfusion (FD-CTP) imaging has demonstrated efficacy in qualitatively accessing the penumbra in acute stroke equivalent to that of magnetic resonance perfusion (MRP). The aim of our study was to evaluate the feasibility of quantifying oligemia in the brain in patients with carotid stenosis.

Ten patients with unilateral carotid stenosis of >70% were included. All MRPs and FD-CTPs were performed before stenting. Region-of-interests (ROIs) including middle cerebral artery territory at basal ganglia level on both stenotic and contralateral sides were used for quantitative analysis. Relative time to peak (rTTP) was defined as TTP of the stenotic side divided by TTP of the contralateral side, and so as relative cerebral blood volume (rCBV), relative mean transit time (rMTT), and relative cerebral blood flow (rCBF). Absolute and relative TTP, CBV, MTT, CBF between two modalities were compared.

For absolute quantitative analysis, the correlation of TTP was highest ($r = 0.56$), followed by CBV ($r = 0.47$), MTT ($r = 0.47$), and CBF ($r = 0.43$); for relative quantitative analysis, rCBF was the highest ($r = 0.79$), followed by rTTP ($r = 0.75$) and rCBV ($r = 0.50$).

We confirmed that relative quantitative assessment of FD-CTP is feasible in chronic ischemic disease. Absolute quantitative measurements between MRP and FD-CTP only expressed moderate correlations. Optimization of acquisitions and algorithms is warranted to achieve better quantification.

(*Medicine* 95(20):e3529)

Abbreviations: AIF = arterial input function, CBF = cerebral blood flow, CBV = cerebral blood volume, FD-CTP = flat-detector CT perfusion imaging, HPS = hyperperfusion syndrome, MCA = middle cerebral artery, MRP = magnetic resonance perfusion, MTT = mean transit time, TTP = time to peak.

Editor: Rani Al-Senan.
Received: January 18, 2016; revised: March 21, 2016; accepted: March 26, 2016.
From the Department of Radiology (C-JL, W-YG, F-CC, S-CH, J-KAL), Taipei Veterans General Hospital; School of Medicine (C-JL, W-YG, F-CC, S-CH), National Yang-Ming University; Department of Biomedical Imaging and Radiological Sciences (S-CH, K-KC, J-KAL), School of Biomedical Science of Engineering, National Yang-Ming University; Siemens Healthcare GmbH (D-ZY), Advanced Therapies, Forchheim, Germany; Siemens Healthcare Ltd. (C-HFW), Advanced Therapies, Taipei, Taiwan.
Correspondence: Sheng-Che Hung, Department of Radiology, Taipei Veterans General Hospital, No. 201, Sec. 2, Shipai Rd., Beitou District, Taipei City , Taiwan 11217 (e-mail: hsz829@gmail.com).
Funding: This research was sponsored by Taipei Veterans General Hospital to Dr. W. Y. Guo (Award number: T1100200) and Dr. Chung Jung Lin (Award number: V104-C-012).
The authors have no conflicts of interest to disclose.

ISSN: 0025-7974
DOI: 10.1097/MD.0000000000003529

INTRODUCTION

Carotid stenosis accounts for 15% to 20% of all cases of stroke.[1] Compared with carotid endarterectomy, carotid stenting is less invasive and has similar primary outcomes of myocardial infarction and death.[2,3] Hyperperfusion syndrome (HPS) is a rare complication of carotid revascularization, including both carotid stenting and endarterectomy. Bilateral carotid stenosis, age, comorbid uncontrolled hypertension, stenotic sinus, and disturbance of the blood–brain barrier have been suggested as playing a role but the exact mechanisms are unclear.[4–7] Nuclear medicine and functional magnetic resonance (MR) have shown that an elevated oxygen extraction fraction and poor cerebral vasoreactivity are risk factors for HPS.[8–10] However, those facilities are of limited timely availability in most hospitals. Perfusion studies have shown that increased cerebral blood volume (CBV), mean transit time (MTT), and time to peak (TTP) are good predictors to identify those who will develop HPS after carotid revasculization.[11,12]

With increased rotation speed and angle of the angiographic C-arm system, sequential CT imaging with an intravenous contrast bolus injection can successfully produce perfusion-like imaging,[13,14] with initial results from animal and human studies demonstrating reliable assessment of cerebral hemodynamic CBV, cerebral blood flow (CBF), MTT, and TTP.[14] Struffert et al confirmed that magnetic resonance perfusion (MRP) and FD-CTP ASPECT scores are comparable for patients with acute strokes.[15] Based on an in-room approach, FD-CTP helps triage patients with larger penumbral areas that may potentially benefit more from endovascular therapy.[16]

Following similar reasoning, we expect that this technique can help interventionists identify patients susceptible to developing HPS after carotid revascularization within the angiosuite, allowing timely management to be initiated. The purpose of our study is to explore the level of agreement between the relative and absolute quantitative measures generated by FD-CTP and MRP in cases of carotid stenosis.

MATERIAL AND METHODS

Patient Selection

Prospectively, we consecutively recruited 10 patients referred to our department for carotid stenting from January to August 2015. The inclusion criterion was patients between 50 and 80 year age with symptomatic unilateral carotid stenosis of

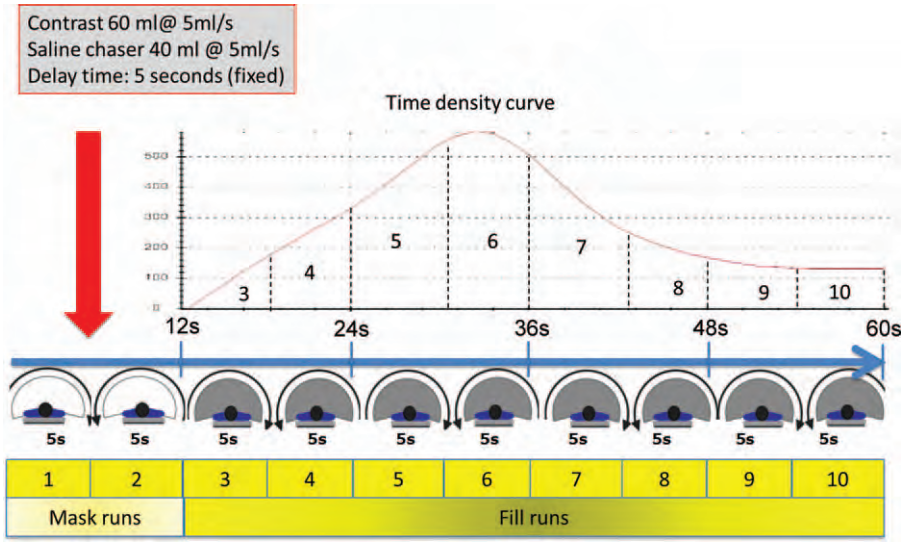

FIGURE 1. Illustration of acquisition of FD-CTP. FD-CTP = flat-detector CT perfusion.

>70% according to NASCET criteria,[17] as this group of patients are expected to benefit from stenting in addition to medication alone. Exclusion criteria were clearance of creatinine <30 mL/min, ejection fraction of left ventricle <40% based on cardiac sonography, or old brain insult with encephalomalacia change. This study was approved by the Institutional Review Board of Taipei Veterans General Hospital. Written informed consent was given by all participants.

MR Perfusion

All MRPs were performed between 1 and 7 days before carotid stenting in the same 1.5 Tesla scanner (Signa HDxt®, GE Healthcare, Milwaukee, WI) with an 8-channel neurovascular coil. Using an echo planar imaging sequence, 70 sequential scans were performed for 7 slices. The temporal resolution was 1 second. Imaging parameters were as follows: 60° flip angle, TR 1000 ms/TE 40 ms, 7-mm section thickness with a 7-mm imaging gap, 240-mm field of view, and 128 × 128 acquisition matrix. A bolus injection of 7 mL godabenate dimeglumine (Multihance®; Bracco, Milan, Italy) was given via the antecubital vein at a rate of 3 mL/s by a power injector (Opistar™ Mallinckrodt Pharmaceuticals, Dublin, Ireland). The MR scan and the bolus started simultaneously. Perfusion Mismatch Analyzer software (version 5.0, ASIST Group, Japan) was used for analysis.[18] To identify an arterial input function (AIF) applicable for both modalities, we selected one located proximal M2. The software automatically determined the venous output function. Standard singular value decomposition was used for the deconvolution algorithm to obtain TTP, CBV, CBF, and MTT values.

Flat-Detector CT Perfusion

All FD-CTPs were obtained immediately before the stenting on the same DSA machine (AXIOM Artis®, Siemens Healthcare, Forchheim, Germany). Each FD-CTP series consisted of 10 C-arm rotations with a duration of about 1 minute. Each rotation took 5 seconds and covered 260°. The gap between 2 rotations was about 1 second. A power injector (Liebel-Flarsheim Angiomat®, Illumena) created a contrast bolus of 60 milliliter contrast (370 mg/dL, Iopamiro, Bracco, Milano, Italy) followed by 40-milliliter normal saline at the rate of 5 mL/s via the antecubital vein. The contrast bolus commenced 5 seconds after FD-CTP acquisition started (Figure 1). The first 2 rotations were used for mask runs; details of the acquisition protocols can be found elsewhere.[14] The datasets were sent to a workstation equipped with a prototype of Dyna CT perfusion (Siemens Healthcare, Forchheim, Germany) for reconstruction. The same principle for selecting the AIF as described earlier for MRP was used for FD-CTP. Likewise, the same deconvolution algorithm used in MRP was used to produce parametric color maps of TTP, CBV, CBF, and MTT.[19–21] We reduced TTP for FD-CTP by 5 seconds from the original values because of the delay for the bolus injection and the scan for subsequent analysis. The process was automatic following the selection of the AIF. The total effective radiation dose for FD-CTP was 4.6 mSv, roughly twice that of the average noncontrast CT of the head.[22] This level is comparable to the multidetector CTP level of 3.6 mSv found in the previous literature.[23,24]

Selection of ROIs

We followed the ASPECT scoring system to access the middle cerebral artery territory at the basal ganglia level of both hemispheres.[25] A neuroradiologist who was not aware of the clinical conditions of the patients manually selected the region-of-interest (ROIs) independently for MRP and FD-CTP. The ROIs contained the insula, M1, M2, and M3 territories (Figure 2). The relative value was defined as the mean value of the stenotic side divided by the mean value of the contralateral side (e.g., $rCBV = Mean_{stenotic\ side}/Mean_{contralateral\ side}$). The ''absolute'' values used in the study were the measured values for TTP, CBV, CBF, and MTT within each ROI.

Selection of ROI in cerebral blood volume map from (A) FD-CTP and (B) MR perfusion in a case with 75% stenosis of left ICA. ROI was manually placed to include anterior MCA territory, middle MCA territory, posterior MCA territory, and insula according to the ASPECT score system.

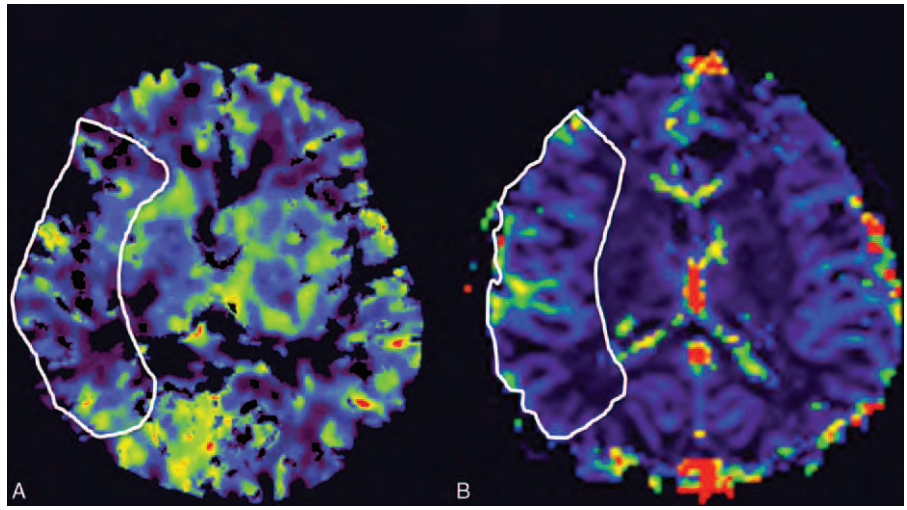

FIGURE 2. Selection of ROI in cerebral blood volume map. ROI = region-of-interest.

Statistical Analysis

Pearson correlations for the relative and absolute measurements of TTP, CBV, CBF, and MTT from MRP and FD-CTP were all explored using SPSS (Version 20, IBM, Armonk, NY). No correlation was defined as $r < 0.25$ or $r > -0.25$; mild correlation was defined as $0.25 < r < 0.50$, or $-0.50 < r < -0.25$); and moderate correlation was defined as $0.50 < r < 0.70$, or $-0.70 < r < -0.50$. Agreement between the two modalities (FD-CTP and MRP) was explored using Bland–Altman analysis. The Wilcoxon signed-rank test was used to test for differences between quantitative measurements of MRP and FD-CTP in 4 perfusion parameters. The threshold for statistical significance for all differences was set at $P < 0.05$.

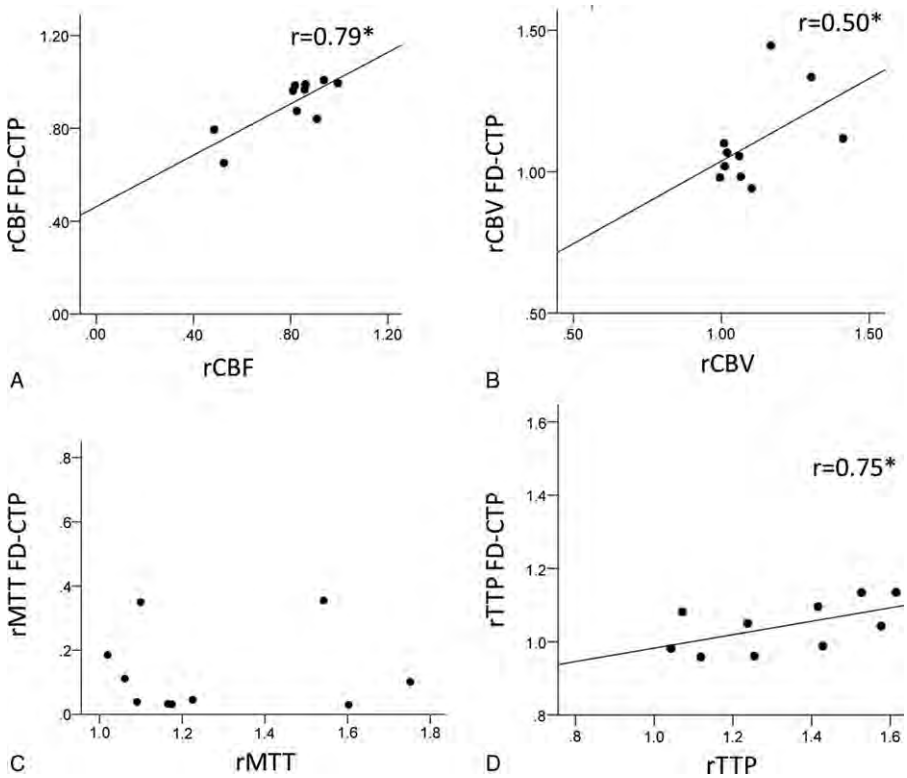

FIGURE 3. Correlation between MRP and FD-CTP relative hemodynamic parameters. (A) *X* axis: rCBF from MRP; *Y* axis: rCBF from FD-CTP. (B) *X* axis: CBV from MRP; *Y* axis: rCBV from FD-CTP. (C) *X* axis: rMTT from MRP; *Y* axis: rMTT from FD-CTP. (D) *X* axis: rTTP from MRP; *Y* axis: rTTP from FD-CTP. *Indicates statistically significant. CBF = cerebral blood flow, CBV = cerebral blood volume, FD-CTP = flat-detector CT perfusion, MCA = middle cerebral artery, MRP = magnetic resonance perfusion, MTT = mean transit time, TTP = time to peak.

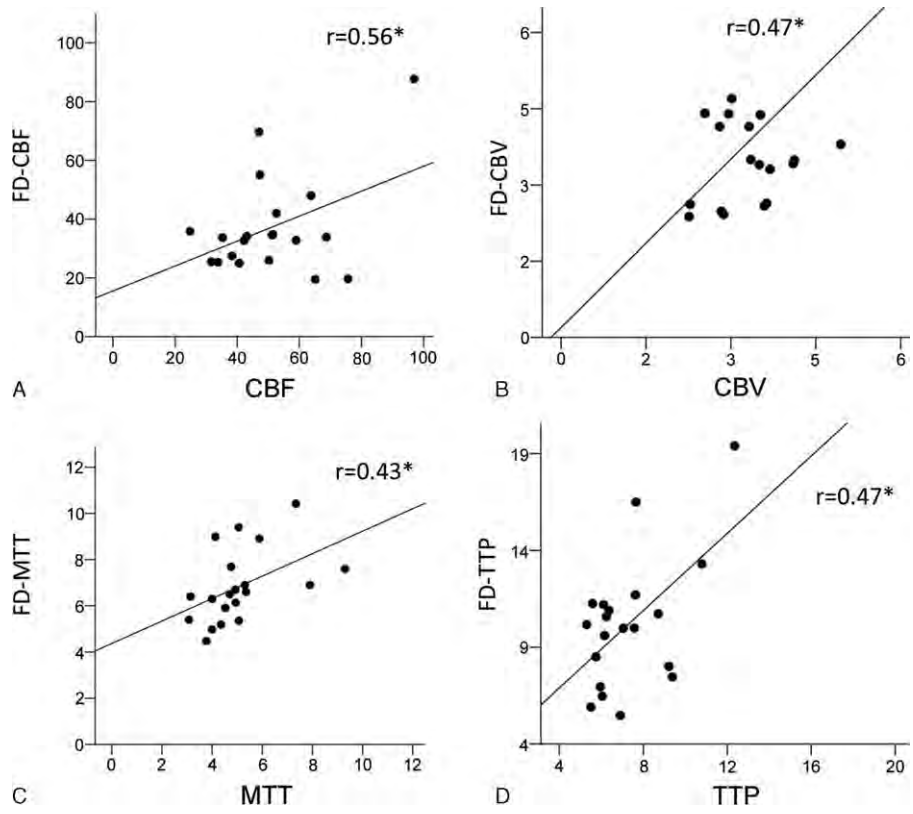

FIGURE 4. Correlation between MRP and FD-CTP quantitative hemodynamic parameters. (A) *X* axis: CBF from MRP; *Y* axis: CBF from FD-CTP. (B) *X* axis: CBV from MRP; *Y* axis: CBV from FD-CTP. (C) *X* axis: MTT from MRP; *Y* axis: MTT from FD-CTP. (D) *X* axis: TTP from MRP; *Y* axis: TTP from FD-CTP. *Indicates statistically significant. CBF = cerebral blood flow, CBV = cerebral blood volume, FD-CTP = flat-detector CT perfusion, MCA = middle cerebral artery, MRP = magnetic resonance perfusion, MTT = mean transit time, TTP = time to peak.

RESULTS

The median age of the 10 patients was 58.5 years, with ages ranging from 35 to 79. The median stenotic degree was 78%. For the relative values, a strong correlation was found in rCBF ($r = 0.79$) and rTTP ($r = 0.75$); only a moderate correlation existed in rCBV ($r = 0.50$) (Figure 3). For the absolute measurements, the correlation of the MRP and FD-CTP absolute values for TTP was moderate ($r = 0.56$), whereas CBV ($r = 0.47$), CBF ($r = 0.43$), and MTT ($r = 0.47$) were all mild (Figure 4). No correlation was found for rMTT values across the two modalities. The Bland–Altman plots for each of the 4 parameters are shown in Figure 5. Differences between the modality values increased slightly as the mean values increased for both CBV and TTP. There was no proportional bias for CBF or MTT. The CBF of FD-CTP (37.17 ± 16.88) was significantly lower than that of MRP (48.73 ± 17.00) ($P < 0.001$); the MTT of FD-CTP (6.58 ± 1.58) was significantly longer than that of MRP (4.84 ± 1.54) ($P < 0.001$). The TTP of FD-CTP (5.47–9.20) was also significantly longer than that of MRP ($P < 0.001$) (Table 1).

DISCUSSION

Despite the small number of patients in our pilot study, our absolute quantitative measurements of MRP were very close to those found in the previous literature.[26] Extracranial carotid stenosis reduced CBF in ipsilateral hemisphere and prolonged MTT and TTP.[27] The change of CBV depended on the severity of stenosis. In cases of 70% to 80% stenosis, CBV remained unchanged (Figure 6). When the degree of stenosis degree exceeds 80%, increased oxygenation extraction cannot compensate the diminished CBF. Therefore, vasodilation of the distal ipsilateral vessels occurs and increases the CBF.[28,29] Parts of the increased CBV results from the recruitment of the collateral circulation and adequate collateral indicates better prognosis in subsequent strokes.[30,31]

TTP was a direct estimation based on the fitted time density curve (TDC) from the voxel of interest in the flat-panel CT imaging. CBV was estimated from the area under the curve. The interval of FD-CTP acquisition is ~5 seconds, which is longer than the MRP scan interval. Goh et al showed that TTP and CBV remain almost unchanged despite the prolonged scan interval; nevertheless, over-estimation of CBF and under-estimation of MTT occurred when the scan interval exceeded 3 seconds.[32] Our FD-CTP used a 5-second scan interval. Although CBV remained constant, both TTP and MTT were prolonged, and CBF values were smaller than those in MRP (Figure 7). We hypothesize that confounding factors other than different intervals intervened.

When using relative values, the correlations for CBF and TTP were strong, CBV values were moderately correlated, and MTT values were only poorly correlated. These findings differ slightly from those in the previous literature.[15] Struffert et al demonstrated that grading the severity of acute middle cerebral artery occlusion by parametric assessment of FD-CTP was reliable except for CBV. In our findings, the correlation for

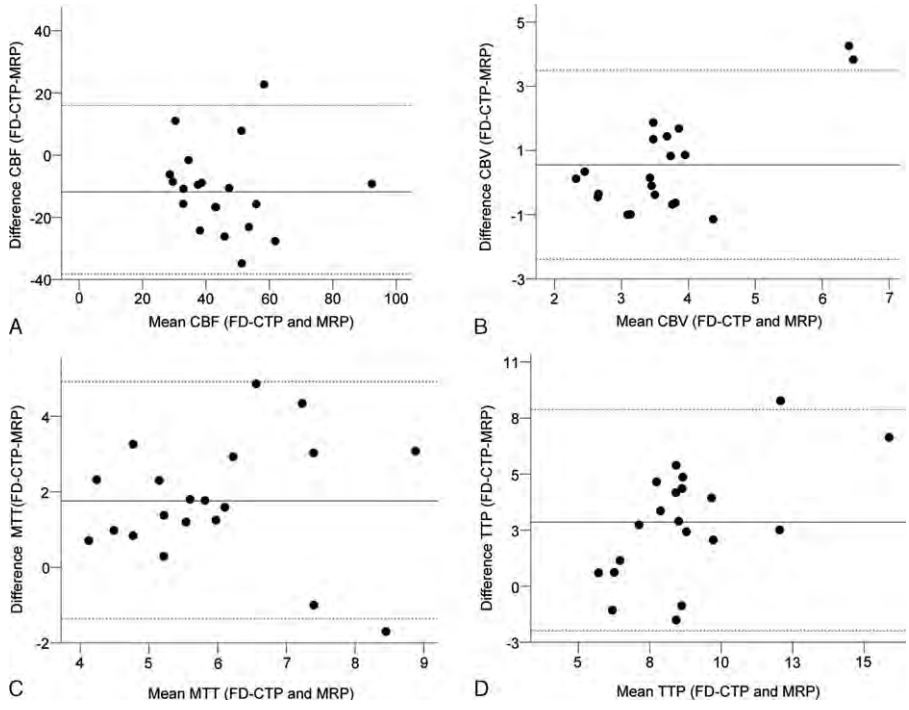

FIGURE 5. Bland–Altman plots between MRP and FD-CTP quantitative hemodynamic parameters. (A) *X* axis: mean CBF from MRP and FD-CTP; *Y* axis: Difference of CBF from MRP and FD-CTP. (B) *X* axis: mean CBV from MRP and FD-CTP; *Y* axis: Difference of CBV from MRP and FD-CTP. (C) *X* axis: mean MTT from MRP and FD-CTP; *Y* axis: Difference of MTT from MRP and FD-CTP. (D) *X* axis: mean TTP from MRP and FD-CTP; *Y* axis: Difference of TTP from MRP and FD-CTP. CBF = cerebral blood flow, CBV = cerebral blood volume, FD-CTP = flat-detector CT perfusion, MRP = magnetic resonance perfusion, MTT = mean transit time, TTP = time to peak.

MTT values was better for direct, absolute MTT than for rMTT. We hypothesize that the changes of MTT were more complicated and had wider variation in stenotic cases than in cases of middle artery occlusion. Using both sides to calculate relative values decreased its stability. In contrast to TTP, CBF, and CBV, using absolute instead of relative MTT values is thus recommended. The mild to moderate correlation between MRP and FD-CTP is not necessarily a result of errors from FD-CTP. MRP values may also include measurement error and the ''gold standard'' for evaluating CBF remains SPECT.[33]

In our FD-CTP workflow, continuous acquisition was done without separating mask and filling runs.[15] Our acquisition time for FD-CTP was 1 minute, similar to the durations of MRPs and CTPs. We also used the fixed delayed method regardless of patient age or vessel condition. We did not encountered situations such as a contrast in the mask run (too late) or termination of acquisition before the concentration started to drop in the superior sagittal sinus (too early). Both above-mentioned conditions would have truncated the TDC and generated enormous bias in the subsequent analysis. Our modified approach made it easier to catch the contrast bolus.[20,34] Each FD-CTP imaging dataset was reconstructed via a 5-second C-arm rotation, making it sensitive to motion artifacts. Fixation of head and patient cooperation are crucial for obtaining images of diagnostic quality.

This is a pilot study and therefore the number of cases was limited. This is a pilot feasibility study and therefore the number of cases was limited. Further larger scale studies with more

TABLE 1. Comparisons of MR Perfusion and Flat-Detector CT Perfusion Values for TTP, CBV, CBF, and MTT

	MR Perfusion		Flat-Detector CT Perfusion		*P* Value
	Median	(Q1–Q3)	Median	(Q1–Q3)	
TTP (s)	6.63	(5.95–7.65)	8	(5.47–9.20)	0.011*
CBV (mL/100 g)	3.42	(2.83–3.69)	3.49	(2.65–4.38)	0.263
CBF (mL/100 g/min)	48.73	(38.32–58.92)	37.17	(25.5–35.86)	0.004*
MTT (s)	4.84	(4.00–5.31)	6.58	(5.40–7.6)	0.001*

CBF = cerebral blood flow, CBV = cerebral blood volume, CT = confidence interval, MR = magnetic resonance, MTT = mean transit time, TTP = time to peak.
Q1: first quartile; Q3: third quartile.
*Statistically significant.

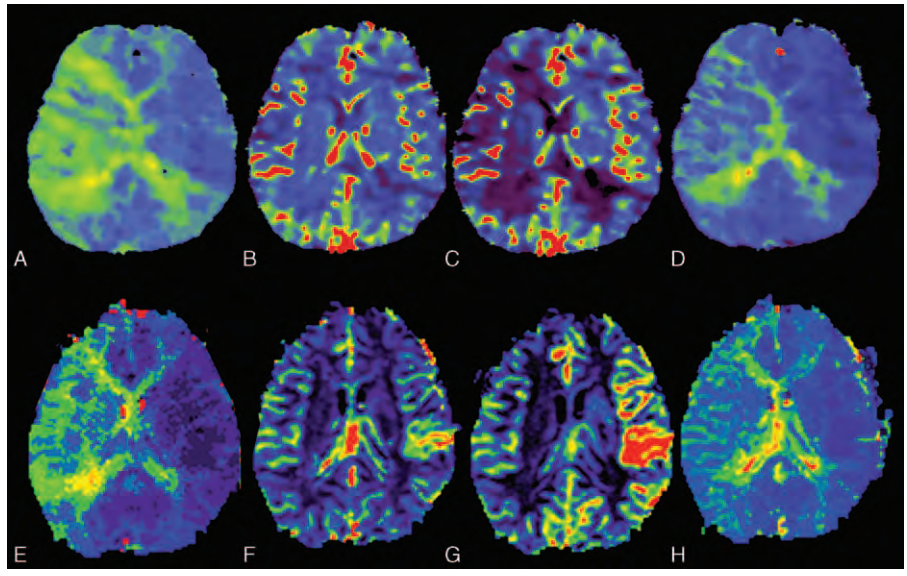

FIGURE 6. Right internal carotid artery of 80% stenosis received FD-CTP and MRP. A 60-year-old male with right internal carotid artery 80% stenosis received FD-CTP (A: TTP, B: CBV; C: CBF; D: MTT) and MRP (E: TTP, F: CBV; G: CBF; H: MTT). The parametric scales were the same for both modalities. Both FD-CTP and MRP demonstrated the similar findings: Prolonged TTP in right MCA territory, equivalent CBV in both sides, decreased CBF in right MCA territory, more evident in watershed areas, and prolonged MTT in right MCA territory. CBF = cerebral blood flow, CBV = cerebral blood volume, FD-CTP = flat-detector CT perfusion, MCA = middle cerebral artery, MRP = magnetic resonance perfusion, MTT = mean transit time, TTP = time to peak.

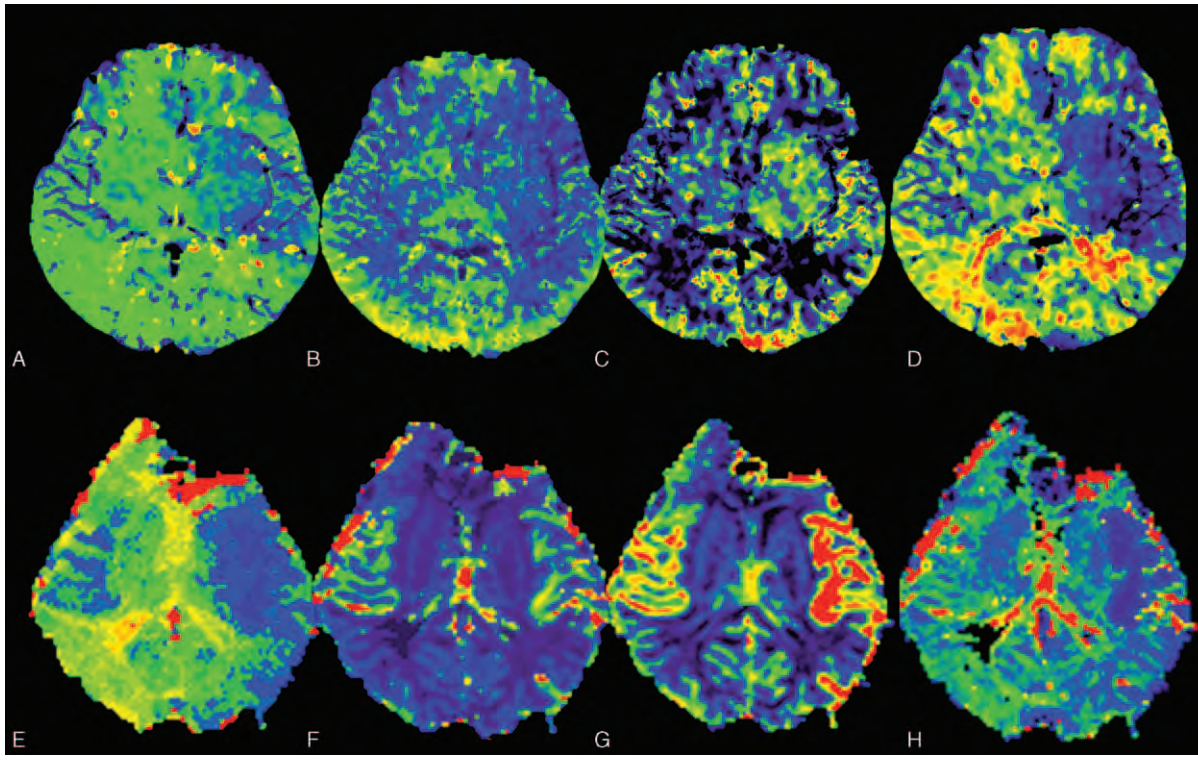

FIGURE 7. Right internal carotid artery of 90% stenosis received FD-CTP and MRP. A 57-year-old male with right internal carotid artery 90% stenosis received FD-CTP (A: TTP, B: CBV; C: CBF; D: MTT) and MRP (E: TTP, F: CBV; G: CBF; H: MTT). The parametric scales were the same for both modalities. In TTP (A & E), both modalities showed similar degrees of prolongation; in MTT (B & F), both modalities showed a similar slight increase in CBV because of severe stenosis. In CBF, FD-CTP showed a more significant decrease in the right MCA territory compared with that in MRP. In MTT, FD-CTP showed a more significant prolongation in the right MCA territory compared with that in MRP. CBF = cerebral blood flow, CBV = cerebral blood volume, FD-CTP = flat-detector CT perfusion, MCA = middle cerebral artery, MRP = magnetic resonance perfusion, MTT = mean transit time, TTP = time to peak.

patients are warranted to validate our initial results. Potential bias caused by physiologic variation of cardiac output and blood pressures exists between the interval between FD-CTP and MRP. Elucidation of the influence upon cerebral hemodynamics of these covariates will further improve the quality of the quantitative measurement. Multi-detector CT perfusion would be ideal for validating FD-CTP. However, the iodine contrast induced nephron toxicity would be a major concern, especially in elderly patients.[35] We also note that a 60-milliliter contrast was adequate for people with normal body mass index. As compared with injection protocols for modern CTP from multidetectors, there is a chance to further decrease contrast volume in slimmer patients.[36,37] Furthermore, in clinical scenarios, relative quantitative assessment is used to determine cerebral vasoreactivity more often than absolute quantitative assessment.

The TDC change of brain parenchyma is ~30 H.U, and FD-CTP is thus more vulnerable to noise. Noise reduction can be achieved by iterative reconstruction and joint bilateral filters.[13] Temporal averaging in FD-CTP produces certain artifacts and these can be mitigated by simultaneous regularization of the time-spatial matrix during reconstruction.[38] Struffert et al proposed evaluating the intracranial vessels reconstructed from FD-CTP to have a roadmap before endovascular treatment.[15] Noninvasive vessel imaging is also important in treating carotid stenosis because some patients have tortuous aortic arches which increase the technique difficulty and complication rates. A single acquisition of FD-CTP to cover the neck and brain vasculature would be of great value but the scan range is too long to cover using present hardware. Providing vascular and perfusion imaging within the angiosuite will facilitate endovascular treatment by shortening the transferal time between diagnostic modalities and the angiosuite.[39,40]

CONCLUSION

The relative measures generated by FD-CTP have proven to be robust for assessing cerebral hemodynamic insufficiency in cases of carotid stenosis. However, the absolute value measurements generated by FD-CTP only achieved moderate correlations with MRP. Further improvement of the accuracy should focus mainly on artifact reduction caused from limited sampling frequency and angles. The approach helps identify patients at higher risks of developing hyperperfusion within the angiosuite, allowing interventionists to take the steps necessary to improve patient safety. Combining diagnostic and interventional facilities within the same room improves treatment results and patient safety.

REFERENCES

1. Chimowitz MI, Lynn MJ, Howlett-Smith H, et al., Investigators W-ASIDT. Comparison of warfarin and aspirin for symptomatic intracranial arterial stenosis. *New Engl J Med.* 2005;352:1305–1316.
2. Groschel K, Schnaudigel S, Pilgram SM, et al. A systematic review on outcome after stenting for intracranial atherosclerosis. *Stroke.* 2009;40:e340–347.
3. Ederle J, Bonati LH, Dobson J, et al., Investigators C. Endovascular treatment with angioplasty or stenting versus endarterectomy in patients with carotid artery stenosis in the Carotid and Vertebral Artery Transluminal Angioplasty Study (CAVATAS): long-term follow-up of a randomised trial. *Lancet Neurol.* 2009;8: 898–907.
4. Ivens S, Gabriel S, Greenberg G, et al. Blood-brain barrier breakdown as a novel mechanism underlying cerebral hyperperfusion syndrome. *J Neurol.* 2010;257:615–620.
5. Ascher E, Markevich N, Schutzer RW, et al. Cerebral hyperperfusion syndrome after carotid endarterectomy: predictive factors and hemodynamic changes. *J Vasc Surg.* 2003;37:769–777.
6. Abou-Chebl A, Yadav JS, Reginelli JP, et al. Intracranial hemorrhage and hyperperfusion syndrome following carotid artery stenting: risk factors, prevention, and treatment. *J Am Coll Cardiol.* 2004;43:1596–1601.
7. Lin C-J, Chang F-C, Tsai F-Y, et al. Stenotic transverse sinus predisposes to poststenting hyperperfusion syndrome as evidenced by quantitative analysis of peritherapeutic cerebral circulation time. *AJNR Am J Neuroradiol.* 2014;35:1132–1136.
8. Iwata T, Mori T, Tajiri H, et al. Predictors of hyperperfusion syndrome before and immediately after carotid artery stenting in single-photon emission computed tomography and transcranial color-coded real-time sonography studies. *Neurosurgery.* 2011;68:649–655discussion 655-646.
9. Hosoda K, Kawaguchi T, Shibata Y, et al. Cerebral vasoreactivity and internal carotid artery flow help to identify patients at risk for hyperperfusion after carotid endarterectomy. *Stroke.* 2001;32: 1567–1573.
10. Chang TY, Liu HL, Lee TH, et al. Change in cerebral perfusion after carotid angioplasty with stenting is related to cerebral vasoreactivity: a study using dynamic susceptibility-weighted contrast-enhanced MR imaging and functional MR imaging with a breath-holding paradigm. *AJNR Am J Neuroradiol.* 2009;30: 1330–1336.
11. Tseng YC, Hsu HL, Lee TH, et al. Prediction of cerebral hyperperfusion syndrome after carotid stenting: a cerebral perfusion computed tomography study. *J Comput Assist Tomogr.* 2009;33: 540–545.
12. Chang C-H, Chang T-Y, Chang Y-J, et al. The role of perfusion computed tomography in the prediction of cerebral hyperperfusion syndrome. *PLoS One.* 2011;6:e19886.
13. Manhart MT, Kowarschik M, Fieselmann A, et al. Dynamic iterative reconstruction for interventional 4-D C-arm CT perfusion imaging. *IEEE Trans Med Imaging.* 2013;32:1336–1348.
14. Royalty K, Manhart M, Pulfer K, et al. C-arm CT measurement of cerebral blood volume and cerebral blood flow using a novel high-speed acquisition and a single intravenous contrast injection. *AJNR Am J Neuroradiol.* 2013;34:2131–2138.
15. Struffert T, Deuerling-Zheng Y, Kloska S, et al. Dynamic angiography and perfusion imaging using flat detector CT in the angiography suite: a pilot study in patients with acute middle cerebral artery occlusions. *AJNR Am J Neuroradiol.* 2015;36:1964–1970.
16. Campbell BC, Mitchell PJ, Kleinig TJ, et al., Investigators E-I. Endovascular therapy for ischemic stroke with perfusion-imaging selection. *New Engl J Med.* 2015;372:1009–1018.
17. North American Symptomatic Carotid Endarterectomy Trial Collaborators. Beneficial effect of carotid endarterectomy in symptomatic patients with high-grade carotid stenosis. *New Engl J Med.* 1991;325:445–453.
18. Kudo K, Sasaki M, Ogasawara K, et al. Difference in tracer delay-induced effect among deconvolution algorithms in CT perfusion analysis: quantitative evaluation with digital phantoms1. *Radiology.* 2009;251:241–249.
19. Fieselmann A, Ganguly A, Deuerling-Zheng Y, et al. Interventional 4-D C-arm CT perfusion imaging using interleaved scanning and partial reconstruction interpolation. *IEEE Trans Med Imaging.* 2012;31:892–906.

20. Ganguly A, Fieselmann A, Marks M, et al. Cerebral CT perfusion using an interventional C-arm imaging system: cerebral blood flow measurements. *AJNR Am J Neuroradiol.* 2011;32:1525–1531.
21. Fieselmann A, Kowarschik M, Ganguly A, et al. Deconvolution-based CT and MR brain perfusion measurement: theoretical model revisited and practical implementation details. *Int J Biomed Imaging.* 2011;2011:467563.
22. Struffert T, Hauer M, Banckwitz R, et al. Effective dose to patient measurements in flat-detector and multislice computed tomography: a comparison of applications in neuroradiology. *Eur Radiol.* 2014;24:1257–1265.
23. Wu T-H, Hung S-C, Sun J-Y, et al. How far can the radiation dose be lowered in head CT with iterative reconstruction? Analysis of imaging quality and diagnostic accuracy. *Eur Riol.* 2013;23: 2612–2621.
24. Smith AB, Dillon WP, Lau BC, et al. Radiation dose reduction strategy for CT protocols: successful implementation in neuroradiology section. *Radiology.* 2008;247:499–506.
25. Pexman JHW, Barber PA, Hill MD, et al. Use of the Alberta Stroke Program Early CT Score (ASPECTS) for assessing CT scans in patients with acute stroke. *AJNR Am J Neuroradiol.* 2001;32: 1534–1542.
26. Lythgoe DJ, Ostergaard L, William SC, et al. Quantitative perfusion imaging in carotid artery stenosis using dynamic susceptibility contrast-enhanced magnetic resonance imaging. *Magn Reson Imaging.* 2000;18:1–11.
27. Soinne L, Helenius J, Tatlisumak T, et al. Cerebral hemodynamics in asymptomatic and symptomatic patients with high-grade carotid stenosis undergoing carotid endarterectomy. *Stroke.* 2003;34:1655–1661.
28. Doerfler A, Eckstein HH, Eichbaum M, et al. Perfusion-weighted magnetic resonance imaging in patients with carotid artery disease before and after carotid endarterectomy. *J Vasc Surg.* 2001;34: 587–593.
29. Kawai N, Hatakeyama T, Okauchi M, et al. Cerebral blood flow and oxygen metabolism measurements using positron emission tomography on the first day after carotid artery stenting. *J Stroke Cerebrovasc Dis.* 2014;23:e55–64.
30. Romero JR, Pikula A, Nguyen TN, et al. Cerebral collateral circulation in carotid artery disease. *Curr Cardiol Rev.* 2009;5: 279–288.
31. Wu B, Wang X, Guo J, et al. Collateral circulation imaging: MR perfusion territory arterial spin-labeling at 3T. *AJNR Am J Neuroradiol.* 2008;29:1855–1860.
32. Goh V, Liaw J, Bartram CI, et al. Effect of temporal interval between scan acquisitions on quantitative vascular parameters in colorectal cancer: implications for helical volumetric perfusion CT techniques. *AJR Am J Roentgenol.* 2008;191:W288–292.
33. Wintermark M, Sesay M, Barbier E, et al. Comparative overview of brain perfusion imaging techniques. *Stroke.* 2005;36:e83–e99.
34. Caroff J, Jittapiromsak P, Ruijters D, et al. Use of time attenuation curves to determine steady-state characteristics before C-arm CT measurement of cerebral blood volume. *Neuroradiology.* 2014;56:245–249.
35. Rosovsky M, Rusinek H. Dose-related nephrotoxicity. *Radiology.* 2006;240:614.
36. Konstas AA, Goldmakher GV, Lee TY, et al. Theoretic basis and technical implementations of CT perfusion in acute ischemic stroke, part 1: theoretic basis. *AJNR Am J Neuroradiol.* 2009;30: 662–668.
37. Konstas AA, Wintermark M, Lev MH. CT perfusion imaging in acute stroke. *Neuroimaging Clin N Am.* 2011;21:215–238.
38. Chen GH, Li Y. Synchronized multiartifact reduction with tomographic reconstruction (SMART-RECON): a statistical model based iterative image reconstruction method to eliminate limited-view artifacts and to mitigate the temporal-average artifacts in time-resolved CT. *Med Phys.* 2015;42:4698–4707.
39. Guo W-Y, Wu Y-T, Wu H-M, et al. Toward normal perfusion after radiosurgery: perfusion MR imaging with independent component analysis of brain arteriovenous malformations. *AJNR Am J Neuroradiol.* 2004;25:1636–1644.
40. Chao A-C, Hsu H-Y, Chung C-P, et al., Group TTTfAIST-AS. Outcomes of thrombolytic therapy for acute ischemic stroke in Chinese patients: the Taiwan Thrombolytic Therapy for Acute Ischemic Stroke (TTT-AIS) study. *Stroke.* 2010;41: 885–890.